Characterization of Anionic/Cationic Sequential IPNs. II. Studies of Swelling, Modulus, and Alternate Phase Staining with CsF and LiI

S. C. HARGEST, J. A. MANSON, and L. H. SPERLING, *Lehigh University, Materials Research Center, Coxe Laboratory #32, Bethlehem, Pennsylvania 18105*

Synopsis

Anionic/cationic interpenetrating polymer networks (IPNs) were synthesized by sequential polymerization from crosslinked polystyrene, PS, as polymer I and crosslinked poly(4-vinyl pyridine), P(4-VP), as polymer II. Ionomeric substitution of the two networks was based on sulfonation and quaternization of the phenyl and pyridine rings, respectively. The swelling, morphological, and dynamic mechanical behavior of ionomeric and unsubstituted IPNs was explored as a function of overall IPN composition. A theoretical analysis of the unsubstituted IPNs via the Thiele–Cohen equation showed that essentially no additional physical or chemical crosslinks were developed in the swollen state. Modulus studies showed that network I tends to dominate the mechanical properties in the bulk state. Swelling studies on the ionomeric IPNs as a function of pH demonstrated a complex change in behavior with the addition of NaCl, possibly due to an ionic screening effect. Electron microscopy involved alternate staining of the anionic and cationic phases using CsF and LiI and showed a two-phase structure, with the possibility of additional phases within phases due to separation of the ionomeric components. Comparison of the two staining techniques yielded strong evidence of a positive/negative–negative/positive phase contrast, depending on the phase being stained. In each case, domains were less than 100 nm (1000 Å), with the domain size decreasing as the P(4-VP) content increased. Also, a phase inversion appeared to occur between 50 and 80% P(4-VP). The dynamic mechanical studies supported the two-phase morphology and gave evidence of significant molecular mixing between the phases.

INTRODUCTION

Interpenetrating polymer networks (IPNs) form a unique class of materials, displaying unusual morphologies and behavior. IPNs may be synthesized in a variety of ways but generally involve mixtures of two or more distinct, crosslinked polymer networks incapable of gross physical separation.[1] The IPNs studied in this work are termed sequential IPNs, synthesized by swelling a crosslinked polymer network (I) with a second monomer (II), plus crosslinking and activating agents, and polymerizing monomer II *in situ*.[2–6]

In the ideal case of mutual solubility, both polymers might be expected to penetrate each other on a molecular scale, each becoming continuous throughout the material. In the more typical case of polymers I and II being chemically different, some degree of incompatibility and phase separation usually results.[4,5,7–10] This phase separation stems from the low entropy of mixing, which causes the enthalpy term to dominate in the Gibbs free-energy relationship.[11,12] The unusual properties of IPNs result from the characteristics of phase sepa-

Journal of Applied Polymer Science, Vol. 25, 469–485 (1980)

0021-8995/80/0025-0469$01.00

ration, such as extent of separation, phase continuity, and phase size and shape.

This paper delineates the synthesis and characterization of anionic/cationic IPNs and their unsubstituted counterparts. By varying the weight ratio of polymer I to polymer II, the synthesis, morphology, swelling behavior, and dynamic mechanical behavior of anionic/cationic IPNs based on sulfonated polystyrene (polymer I) and quaternized poly(4-vinyl pyridine) (polymer II) were examined.

Selective highlighting of the anionic or cationic phases using CsF or LiI staining reveals novel views of the morphology under the electron microscope. Ideally, transmission electron micrographs of totally incompatible, two-phased materials should produce a positive/negative–negative/positive contrast, depending on the phase being stained. For partly compatible materials, overlaps and gradations of staining should be observed. Also, the possibility that anionic/cationic IPNs may exhibit additional phases exists, due to phase separation of the ionomeric and unsubstituted portions of the two polymers. Evidence supporting both of these possibilities will be presented.

Swelling studies concentrated on the effects of solvent pH on the ionomeric IPNs and on several theoretical predictions of the swelling behavior of the unsubstituted IPNs. Dynamic mechanical spectroscopy (DMS) of the unsubstituted IPNs was used to determine the extent of molecular mixing and phase separation between the two polymers.

THEORY

Swelling and Extraction

For single polymer networks, the Flory–Rehner[13] equilibrium swelling equation has long been used to describe the relationship between the extent of swelling and crosslink density of rubbery materials. The Flory–Rehner equation takes into account the enthalpy and entropy of mixing network chains and solvent, and the elastic retractive forces of the network. Rntly, Thiele and Cohen[14] derived a corresponding equation for homo-IPNs, in which network I is preswollen by network II and polymers I and II are identical except in their crosslink densities,

$$\ln(1 - v_1 - v_2) + v_1 + v_2 + \chi_s(v_1 + v_2)^2 = -V_s N_1' \left(v_1^{1/3} - \frac{v_1}{2}\right) - V_s N_2' \left(v_2^{0\,2/3} v_2^{1/3} - \frac{v_2}{2}\right) \quad (1)$$

where v_1 and v_2 are the volume fractions of polymers I and II in the swollen state, v_2^0 is the volume fraction of polymer II in the unswollen state, V_s is the molar volume of the solvent, χ_s is the polymer–solvent interaction parameter (to be discussed later), and N_1' and N_2' are the crosslink densities of the homopolymer networks, in moles/cm^3, as determined by the Flory–Rehner equation.[13]

Siegfried et al.[15] modified the Thiele–Cohen equation through the addition of a thermoelastic front factor to account for internal energy changes due to swelling.[15–18] The modified version reads

$$\ln(1 - v_1 - v_2) + v_1 + v_2 + \chi_s (v_1 + v_2)^2 = -V_s N_1' \left(\frac{1}{v_1^0}\right)^{2/3} \left(v_1^{1/3} - \frac{v_1}{2}\right) - V_s N_2' \left(v_2^{0\,2/3} v_2^{1/3} - \frac{v_2}{2}\right) \quad (2)$$

where $(1/v_1^0)^{2/3}$ in the first term on the right represents the energetic consequences of chain deformation and v_1^0 is the volume fraction of polymer I in the unswollen state.

In the derivation of both the modified and unmodified versions of the Thiele–Cohen equation, the polymer–solvent interaction parameter χ_s was assumed to be identical for both polymers. Since the equations originally dealt with homo-IPNs, a simple average of the two χ values was assumed for χ_s for the present case:

$$\bar{\chi}_s = w_1\chi_1 + w_2\chi_2 \quad (3)$$

where $\bar{\chi}_s$ is the averaged interaction parameter for the IPN, w_1 and w_2 are the weight fractions of polymers I and II, respectively, and χ_1 and χ_2 are the interaction parameters for homopolymers I and II, respectively. Equation (3), while general, would be expected to yield more accurate results when the solubility parameter of the solvent lies halfway between those of the two polymers, or else lies far to one side or the other of the values for both polymers.

In addition to the data collected by the authors, a brief study of the swelling data of Lipatov et al.[3,19] provided an interesting comparison. Lipatov and coworkers examined the swelling behavior of IPNs consisting of polyurethane (polymer I) and styrene–divinylbenzene copolymer (polymer II) by varying the wt % of DVB in polymer II, the ratio of polymer I to polymer II, and filler content. Analysis of the Lipatov et al.[3,19] data, in conjunction with the present data, has yielded further information concerning the questions of network I domination in IPN behavior and the possible addition of new physical crosslinks during IPN formation.[15]

Swelling studies on the ionomeric IPNs have yielded the polymer–solvent interactions due to the ionic components.[20] Structurally, the ionic portions of the networks resemble ion exchange resins and ionomers.[21–26] Previous studies of anionic/cationic IPNs based on PS and P(4-VP) examined swelling as a function of solvent pH and NaCl concentration.[27] A possible theoretical approach to analyze the ionic interactions uses the empirical correlations proposed by Drago[28] involving the acid–base interactions to predict polar and hydrogen-bonding effects.

Electron Microscopy

Transmission electron microscopy (TEM), coupled with dynamic mechanical spectroscopy (DMS), has become a primary tool in characterizing multiphase polymer systems.[29] Electron microscopy shows the phase domain sizes and shapes, while DMS shows more clearly the extent of molecular mixing.[11] Although phase characteristics of ionomers have been studied using the OsO_4 staining method,[30] for TEM studies, ionic polymers are generally self-staining and do not require additional staining with OsO_4.[31,32] Ion exchange between ionic polymers and salts containing heavy ions, such as cesium or rubidium, has already been used to highlight the ionic phases.[26,33–35] In this work, CsF and

LiI were used to highlight the anionic and cationic phases, respectively. The actual staining reactions involved are as follows:

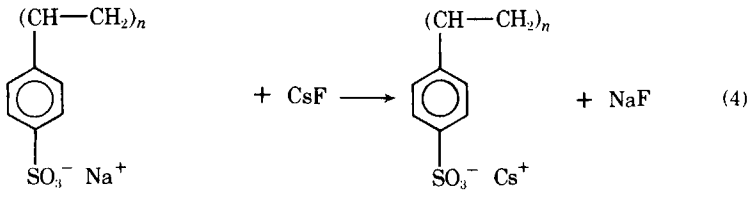

(4)

sulfonated polystyrene

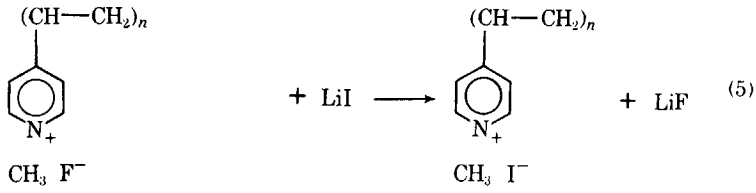

(5)

quaternized poly(4-vinyl pyridine)

In the ideal case, IPNs with the anionic or cationic phases alternately stained would be expected to portray a positive/negative–negative/positive contrast, yielding more information than either staining salt alone.

A semiempirical equation derived by Donatelli et al.[36,37] was used to predict the domain sizes of the discontinuous phase:

$$\frac{\nu_1}{C^2K^2}\left(\frac{\nu_1}{1-W_2}+\frac{2}{M_1}\right)D_2^3+\left(\frac{W_2}{M_2}-\frac{\nu_1}{2}\right)D_2=\frac{2\gamma W_2}{RT} \tag{6}$$

where ν_1 is the crosslink density of polymer I; M_1 is the primary molecular weight of polymer I; D_2 is the domain size of the discontinuous phase; M_2 is the molecular weight of polymer II; W_2 is the weight fraction of polymer II; γ is the interfacial energy between polymers I and II; $K = r_0/M_1^{1/2}$, which is a constant; and T is the absolute temperature. C is a constant, approximately equal to $2^{1/2}$, which assumes that each polymer II domain is surrounded by an average of four polymer I chain segments. Donatelli et al.[36,37] employed a thermodynamic approach to develop eq. (6), taking into consideration the free-energy change for polymer II domain formation. The polymer II domain size depends inversely on the crosslink density of polymer I and also on the interfacial energy and overall composition.

Through appropriate substitutions and algebraic manipulations, eq. (6) simplifies to

$$D_2=\frac{2\gamma W_2}{RT\nu_1\left(\dfrac{1}{1-W_2}-\dfrac{1}{2}\right)} \tag{7}$$

which contains no arbitrary constants. [Equation (7) corrects an algebraic error in the original equation proposed by Donatelli et al.[36,37].]

Dynamic Mechanical Spectroscopy

As previously mentioned, DMS provides information on the compatibility of two polymers and extent of molecular mixing between the phases. In the absence of molecular mixing, two distinct glass transitions will occur, each phase retaining the T_g of its pure homopolymer. As molecular mixing increases, the glass transitions shift toward each other and broaden, with a single transition occurring in the limit of total compatibility.[2,38,40] The actual extent of molecular mixing can be calculated by comparing the observed T_g of each polymer phase with that of its respective homopolymers. The random copolymer equation can be used to estimate each phase composition[41]:

$$T_g = w_1 T_{g_1} + w_2 T_{g_2} \tag{8}$$

where

$$w_1 + w_2 = 1 \tag{9}$$

T_g is the glass transition of the phase under consideration; w_1 and w_2 are the weight fractions of polymers I and II, respectively; and T_{g_1} and T_{g_2} are the glass transitions of polymers I and II, respectively.

EXPERIMENTAL

Synthesis and Elemental Analysis

The synthesis of the anionic/cationic IPNs involved four basic steps. Styrene with 1% divinyl benzene (DVB) and 0.4% benzoin was first photopolymerized via ultraviolet (UV) radiation between two glass plates separated by a polyethylene gasket to form polymer network I. Second, the polystyrene was swelled with a predetermined amount of 4-vinyl pyridine (monomer II) containing 1% DVB and 0.4% benzoin. The 4-vinyl pyridine, obtained from the Aldrich Chemical Company, was vacuum distilled at a pressure of 1700 Pa (13 mm Hg) prior to use. Following swelling, the 4-vinyl pyridine was also polymerized *in situ* with the UV source.

The third step introduced the cationic charges to the IPN by quaternization of the pyridine rings. The IPN was swelled to equilibrium in a chloroform solution containing 6% methylfluorosulfonate by volume. The quaternization reaction was allowed to take place at room temperature for 40 min.

Finally, sulfonation of the polystyrene phenyl rings placed the anionic charges in the IPN. The IPN was swelled in a chloroform solution containing 6% chlorosulfonic acid by volume for 40 min at room temperature, followed by swelling in a 1% aqueous NaOH solution for 10 min. Rinses with dilute HCl and deionized water removed excess reactants. The final anionic/cationic IPN was then based on poly(sodium styrene sulfonate) and poly(4-vinyl-*N*-methyl pyridinium fluoride).

Portions of the homopolymers, IPNs, and ionomeric materials were dried and subjected to elemental analysis* for carbon, hydrogen, nitrogen, sulfur, sodium, and halides (both chlorine and fluorine combined). After allowing for oxygen content, a 20/80 PS/P(4-VP) IPN analyzed to be 45% quaternized and 85% sul-

* Elemental analysis performed by Robertson Laboratories, Florham Park, N.J.

fonated. In addition, two PS and two P(4-VP) homopolymer samples were subjected separately to quaternization or sulfonation reactions to determine the extent of substitution and any cross reactions. One PS sample analyzed to be 97% sulfonated, and the other appeared to be 16% quaternized, based on halide analysis. Since quaternization of the phenyl ring is impossible, the possibility of either fluorination or fluorosulfonation of the ring was raised. However, the elemental analysis showed the sample to contain no sulfur; fluorination of the phenyl ring appears to be the more probable explanation.

Analysis of the P(4-VP) samples revealed them to be 74% quaternized and 29% sulfonated, respectively. This second cross reaction of actual sulfonation probably decreased the contrast in the morphological studies below.

In the presence of salt water, the ionomeric IPNs showed a strong affinity for salt ions, according to chlorine analysis. For example, after extended swelling in 0.3% NaCl solution (followed by soaking in distilled water) elemental analysis showed the IPNs to contain over 200% more chloride than before swelling.

Instrumental

Characterization studies on both the ionomeric and unsubstituted IPNs included (1) swelling and extraction, (2) transmission electron microscopy, and (3) dynamic mechanical spectroscopy. Swelling and extraction studies on both the ionomeric and unsubstituted IPNs were carried out in petri dishes using deionized water, 1% aqueous NaCl, and chloroform as solvents.

A study of the 10-sec shear modulus versus degree of swelling was also carried out, using a Gehman torsional stiffness tester.[42] Deionized water at a neutral pH was used as a solvent with modulus measurements taken at various degrees of swelling from an equilibrium condition to complete dryness.

Transmission electron microscopy on the ionomeric IPNs was performed on a Phillips EM300 electron microscope with a high-resolution stage. Samples were highlighted and "stained" by swelling in 4% solutions of either CsF or LiI for 48 hr. The samples were then imbedded in an epoxy resin and sectioned to a thickness of 40–60 nm (400–600 Å) using a Porter–Blum MT-2 ultramicrotome equipped with a diamond knife.

Dynamic mechanical studies on unsubstituted IPNs were made using a Rhevibron DDV-II unit operating at a frequency of 110 Hz over a temperature range of 50–170°C. The heating rate used was 1°C/min.

RESULTS

Swelling and Extraction

The swelling behavior of the unsubstituted IPNs and homopolymers was examined by equilibrium swelling in chloroform. Using the Flory–Rehner equation, the network chain concentrations N of the homopolymer polystyrene and poly(4-vinyl pyridine) networks were estimated to be 8.5×10^{-5} and 7.9×10^{-5} mole/cm^3, respectively. Figures 1 and 2 show values of v (or $v_1 + v_2$), determined experimentally, versus v predicted by both the unmodified and modified Thiele–Cohen equations, eqs. (1) and (2), respectively, for six different IPN compositions. The modified equation data (Fig. 2) parallels the theoretical line

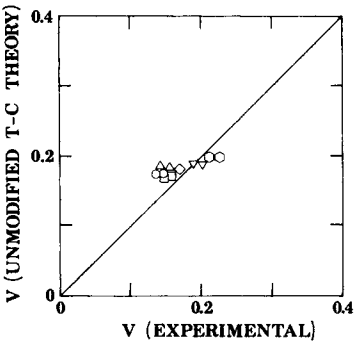

Fig. 1. Quantity v, determined experimentally, versus v, as predicted by the unmodified Thiele–Cohen equation, for unsubstituted IPNs. PS/P(4-VP) = 76/24 (□), 72/28 (○), 61/39 (◇), 58/42 (△), 43/57 (▽), 20/80 (○).

closely, differing by an approximately constant value for all compositions, while the unmodified equation data (Fig. 1) intersect the theoretical line at a composition of approximately 40% PS and 60% P(4-VP). Experimentally, v increased as the wt % of P(4-VP) increased. Both equations predicted this general trend, but the modified equation predicted the rate of increase of v with increasing P(4-VP) content more accurately in that the data parallels the theoretical line.

If new physical or chemical crosslinks were added during IPN formation, the data would be expected to shift to the right of the theoretical line.[15] Figures 1 and 2 demonstrate that, in general, no new physical or chemical crosslinks appeared substantially during IPN formation. Examination of the data does yield a response to the question of network I domination. Network I domination occurs when polymer network I controls and governs the swelling and mechanical behavior of the material. Network I domination is indicated when the swelling data become insensitive to network II composition.[15] The experimental values of the quantity v show nearly the predicted variation with changing composition, especially for the modified Thiele–Cohen equation. Thus, the present swelling data do not indicate any domination of network I in the swollen state.

A similar analysis on the data obtained by Lipatov et al.[3,19] provided some enlightening results. The results for 2 and 3% DVB are summarized in Figure

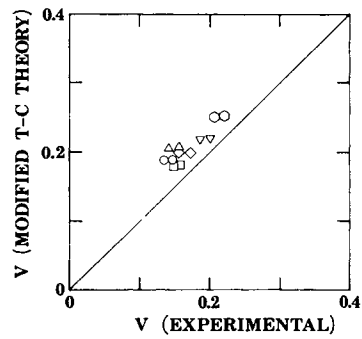

Fig. 2. Quantity v, determined experimentally, versus v, as predicted by eq. (2), for unsubstituted IPNs. PS/P(4-VP) = 76/24 (□), 72/28 (○), 61/39 (◇), 58/42 (△), 43/57 (▽), 20/80 (○).

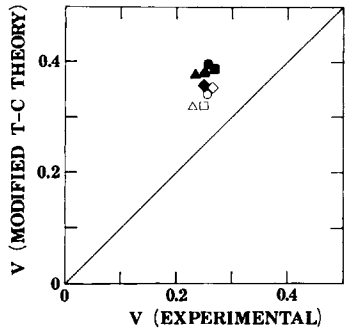

Fig. 3. Analysis of the Lipatov et al. data using eq. (2). Polymer I is polyurethane and polymer II is styrene–DVB copolymer. Open symbols represent 2% DVB and closed symbols represent 3% DVB in polymer II. Polymer I/polymer II, filler content: 78/22 (○), 0%; 79/21 (□), 0%; 85/15 (△), 0%; 68/32 (◇), 1%; 76/24 (●), 0%; 78/22 (■), 0%; 81/19 (▲), 0%; 75/25 (◆), 1%; 60/40 (▲), 1%.

3 using eq. (2). (The unmodified Thiele–Cohen equation yielded substantially the same appearance as Fig. 3.) In all cases, the data lie above the theoretical line, indicating an experimentally greater degree of swelling than predicted, as was the case in Figure 2. In general, the deviations from the theoretical line also increased with increasing DVB content for the data from Lipatov et al. The modified equation was slightly more accurate for Lipatov's data at 0% filler, while at 1% filler the unmodified version provided better predictions.

Concerning network I domination, Lipatov's data show relatively small variations in the experimental v values with substantial variations in the theoretical predictions, suggesting that the crosslink level of network I dictates the material's swelling behavior regardless of the crosslink level of network II. Thus, Lipatov's data do suggest a modest domination of network I over network II, for his system. A similar analysis by Siegfried et al.[15] involving polystyrene/polystyrene homo-IPNs indicated at most a slight domination of network I in the swollen state but a substantial level of domination in the solid state.

Swelling studies on the ionomeric IPNs were performed as a function of pH for four IPN compositions. The swelling fluids used were deionized water containing 0 and 1% NaCl. The pH of the fluid was varied from 2 to 12 by adding small amounts of concentrated NaOH or HCl. Figures 4 and 5 show the results of the swelling studies in 0 and 1% NaCl. In the absence of NaCl (Fig. 4), one can see a minimum occurring in v (or $v_1 + v_2$, using the Thiele–Cohen notation) corresponding to a maximum in swelling, at a neutral to slightly basic pH for all four compositions. In addition, the quantity v increases as the wt % of P(4-VP) increases in the IPNs. Apparently, the sulfonated PS swells to a greater extent than quaternized P(4-VP), with no NaCl present.

With 1% NaCl in the solvent, different swelling behavior results, as shown in Figure 5. For IPNs rich in PS, a minimum occurs again in the quantity v although not necessarily at an approximately neutral pH. However, for compositions rich in P(4-VP), a maximum occurs in the quantity v at a slightly acidic pH, corresponding to a minimum in swelling. Once again, sulfonated PS appears to swell more than quaternized P(4-VP). The difference in swelling behavior upon adding NaCl may be attributable to the higher ion concentration in the solvent. In a separate study, Lopatin and Newey[43] investigated the swelling behavior of sulfonated (polystyrene–polyisoprene–polystyrene) block copolymers

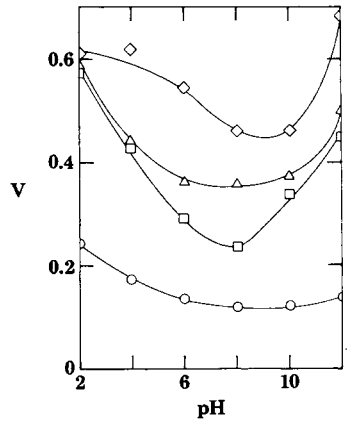

Fig. 4. Quantity v, determined experimentally, as function of pH for ionomeric IPNs. Swelling fluid was deionized water containing 0% NaCl. PS/P(4-VP) = 72/28 (○), 60/40 (□), 39/61 (△), 20/80 (◇).

in water and NaCl solution. They found that the swelling decreased with the addition of NaCl and attributed it to a screening effect caused by the added salt, acting on the mutual electrostatic repulsions between the fixed ion within the network. It is possible that a similar screening effect is causing the different swelling behavior in Figure 5.

For swelling extents short of equilibrium, the modulus depends on the quantity of water imbibed, as the latter behaves as a plasticizer. Figure 6 shows a plot of the 10-sec shear modulus ($3G_{10}$) at room temperature versus v for an ionomeric IPN with an overall composition of 20/80 PS/P(4-VP). The polymer softens rapidly in the range of the quantity v between 0.7 and 0.9, which probably results from the lowering of T_g by plasticization. For values of v lower than 0.7, a rubbery plateau appears. The modulus (from Gehman tests) of the dry ionomeric IPN at room temperature (5×10^{10} Pa) is considerably higher than that of the unsubstituted IPNs (2×10^9 Pa), as measured by DMS (below). The ionomeric IPNs became very fragile and brittle upon complete drying, while the unsubstituted IPNs were not nearly as difficult to handle.

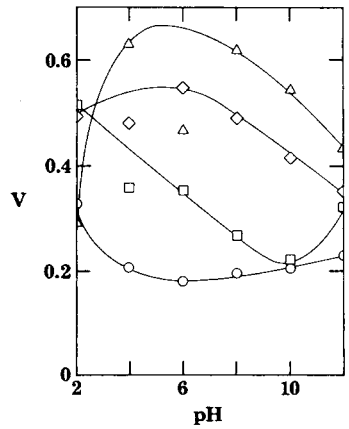

Fig. 5. Quantity v, determined experimentally, as function of pH for ionized IPNs. Swelling fluid was deionized water containing 1% NaCl. PS/P(4-VP) = 72/28 (○), 60/40 (□), 39/61 (△), 20/80 (◇). Different swelling behavior results with the addition of NaCl.

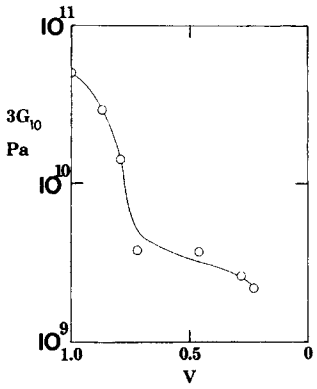

Fig. 6. Ten-sec shear modulus ($3G_{10}$) as function of the degree of swelling for an ionomeric IPN (PS/P(4-VP) = 20/80). The water in the system acts as a plasticizer, causing a rapid softening in the range of υ = 0.9–0.7.

Dynamic Mechanical Spectroscopy

The DMS behavior of the unsubstituted IPNs was studied as a function of temperature and overall IPN composition at 110 Hz. Figure 7 shows the storage (E') and loss (E'') moduli for PS and P(4-VP) homopolymers (dashed and solid lines, respectively) and three IPNs (circles, squares, and triangles). The PS and P(4-VP) homopolymers exhibit single glass transitions at 102 and 136°C, respectively. The storage modulus for each IPN shows two identifiable transitions, each indicative of the T_g of its respective polymer phase. However, there is also a pronounced inward shift of each phase's transition from that of its homopolymer, as shown in Figure 7 and Table I, indicating significant molecular interpenetration and partial compatibility.

While the presence of two transitions for each IPN indicates phase separation of the PS and P(4-VP) networks, the shifting of the T_g values with changing IPN composition (Table I) suggests that the system is not at equilibrium with regard to the classical phase diagram. At the same temperature, all two phase systems at equilibrium must have the same composition within each phase.

Using eqs. (8) and (9), the actual extent of molecular mixing can be calculated

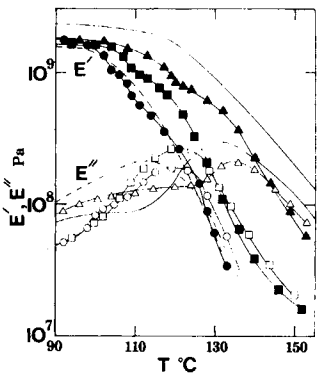

Fig. 7. Temperature dependence of storage modulus E' and loss modulus E'' at 110 Hz for unsubstituted IPNs and homopolymers. PS/P(4-VP) = 100/0 (- -), 76/24 (●, ○), 58/42 (■, □), 20/80 (▲, △), 0/100 (—).

TABLE I
Phase Composition Via DMS

Overall composition PS/P(4-VP)	Glass temperatures, °C		Calculated phase composition	
	T_G(PS)	T_G(P(4-VP))	%P(4-VP) in PS	%PS in P(4-VP)
100/0	102	—	—	—
76/24	102	120	0.00	0.47
58/42	106	119	0.12	0.50
18/82	115	135	0.39	0.03
0/100	—	136	—	—

from the shifts in T_g. The results are also shown in Table I. For all IPN compositions there appears to be significant molecular mixing between the phases, ranging up to 50% in extent. Since the IPN T_g values indicate continuous changes in phase compositions, it must be emphasized that the materials are not at thermodynamic equilibrium.

Electron Microscopy

Figure 8 shows two series of transmission electron micrographs of ionomeric IPNs with four different overall compositions, PS/P(4-VP) = 76/24, 58/42, 50/50, and 20/80. Series I, Figures 8(a)–8(d), is stained with CsF which causes the sulfonated PS phase to appear dark. Series II, (Figures 8(e)–8(h), is stained with LiI which selectively darkens the quaternized P(4-VP) phase. In general, each micrograph exhibits a complex cellular structure, indicative of phase separation within the IPNs. Figure 8(a) shows a cellular morphology with the continuous phase rich in PS and the inner cells primarily P(4-VP). Phase domains are on the order of 60–80 nm (600–800 Å). Figure 8(b) shows a similar cellular structure; domains of P(4-VP) dispersed in a continuous PS matrix. This composition yields phase domains of 35–50 nm (350–500 Å). These smaller domains, appearing much darker, could be a third phase containing a much higher ion concentration. Some suggestion of this triple phase separation can also be seen in Figure 8(a). Figure 8(c) also shows the same type of morphology, with phase domains of 30–40 nm (300–400 Å). The midrange compositions, PS/P(4-VP) = 58/42, 50/50, give some evidence of dual-phase continuity. When the IPN composition becomes rich in P(4-VP), a different cellular arrangement results, as in Figure 8(d). A two-phase cellular structure exists; the continuous phase, however, is P(4-VP), with darker domains of PS throughout. The PS domains are 10–20 nm (100–200 Å) in diameter. Apparently a phase inversion has taken place between 50 and 80% P(4-VP), with P(4-VP) becoming the more continuous component.

Series II, stained with LiI, shows the same general morphological features as series I, although in a different manner. Figure 8(e) has the same composition as Figure 8(a), but the P(4-VP) phase is stained dark. The P(4-VP) phase, with domains 70–80 nm (700–800 Å) in diameter, is dispersed within the PS phase. Again, the same type of structure is shown in Figure 8(f) with a domain size of 40–60 nm (400–600 Å). This micrograph does not show the triple-phase separation as clearly as its compositional analog, Figure 8(b). Figure 8(g) has phase domains on the order of 30–40 nm (300–400 Å), similar to Figure 8(c). Again,

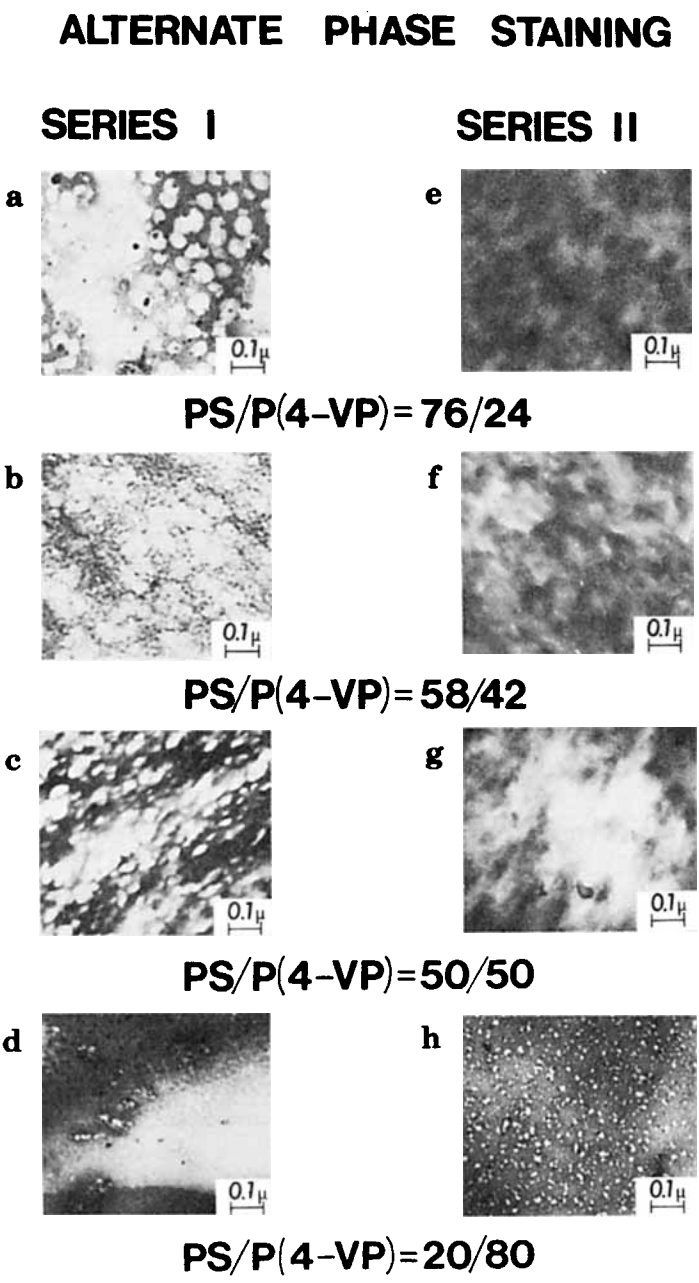

Fig. 8. High-magnification electron micrographs of ionized IPNs, PS/P(4-VP) = 76/24, 58/42, 50/50, 20/80. Series I (CsF stain) shows sulfonated PS as the dark phase, while series II (Li stain) shows quaternized P(4-VP) as the dark phase. Comparing series I and II suggests a complementary stain. Domain sizes decrease as the P(4-VP) content increases, with a phase inversion occurring between 50 and 80% P(4-VP).

the midrange compositions show aspects of dual-phase continuity. As with the CsF-stained series, staining with LiI shows some type of phase inversion to occur with P(4-VP)-rich compositions. Figure 8(h) shows a dark, continuous P(4-VP) phase with lightly colored, discontinuous PS domains 10–20 nm (100–200 Å) in diameter. The discontinuous phase domain sizes, determined from both series of electron micrographs, are plotted in Figure 9. Also plotted are the theoretical values from eq. (7). Except for the 80/20 composition, agreement between theory[37] and experiment staining techniques agree surprisingly well, and both indicate a systematic decrease in domain size with increasing amounts of P(4-VP).

In comparing the left and right portions of Figure 8, each IPN composition shows evidence of a complementary contrast, depending on the phase being stained. For example, consider the composition containing 76% PS and 24% P(4-VP), Figure 8(a) and 8(e). When stained with CsF, P(4-VP) phases (light colored) are observed to be dispersed in a continuous PS phase (dark colored). When LiI is used, an approximate contrast inversion is observed; P(4-VP) phases (light colored) being dispersed in a dark-colored PS matrix. In each case, the P(4-VP) phase domains are on the order of 60–80 nm (600–800 Å) in diameter. Suggestions of this positive/negative–negative/positive change in contrast can be seen with each IPN composition. Each IPN shows phase domain sizes consistent with those of its analog. The rather sharp phase boundaries, especially 8(a), and 8(e), 8(d), and 8(h), suggest that however much mixing occurs within a phase, the composition changes abruptly at the phase boundaries.

DISCUSSION

In each micrograph in Figure 8, the structural features of the cellular morphology are evident, although not extremely clear in some cases. This lack of clarity may result from several factors: (1) As shown by the DMS studies, there is a significant amount of molecular mixing within each phase between the two polymer networks. Such intimate mixing of the phases would cause the morphological features to appear less distinct. (2) In addition, the elemental analysis performed on the ionomeric homopolymers showed that significant extents of cross reaction took place. Since the staining techniques depend on the location

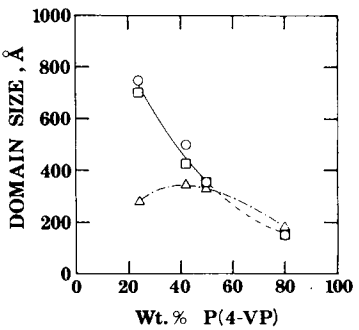

Fig. 9. Domain size of the discontinuous phase as function of P(4-VP) content. Circles represent LiI staining, squares represent CsF staining, and triangles represent predictions made by eq. (7). Dashed line indicates that a phase inversion has occurred between 50 and 80% P(4-VP), with PS becoming the discontinuous phase.

TABLE II
Predicted and Experimental Phase Domain Sizes

PS / P(4-VP) (W_1/W_2)	Phase domain sizes, Å	
	Predicted [eq. (7)]	Experimental (Fig. 8)
76/24	270	700–800
58/42	325	400–600
50/50	316	300–400
20/80	169	100–200

and concentration of the ionic charges, the cross reactions will also tend to reduce the contrast of the micrographs. (3) The effectiveness of the staining techniques is a function of the concentration of ionic groups within the IPN. Significant variation in ionic group concentrations will affect the degree of staining and the clarity of the micrographs. (4) Most importantly, the gradations of staining observed, and the lack of exact positive/negative contrasts, indicate slight extents of overlapping or intermediate composition. These figures show how one polymer diminishes and the other is augmented in concentration at the phase domain boundaries.

The dynamic mechanical studies indicated significant molecular mixing between the two polymers, while the electron micrographs showed a cellular structure (<1000 Å) at all compositions. The electron micrographs showed a decrease in the domain size with increasing P(4-VP) content and showed a phase inversion to occur when P(4-VP) became the majority component.

Using eq. (7) enables the theoretical values of D_2 to be compared with the experimental values obtained from Figure 8 (see Table II). The results are also plotted in Figure 9. Since a value of $\gamma = 10$ dynes/cm gave the best agreement with the experimental results, this value was assumed throughout. In general, the agreement between the experimental and predicted domain sizes is reasonably good, with the exception of $W_2 = 0.24$ [24% P(4-VP)]. The simplified Donatelli equation predicts the same systematic decrease in domain size as shown by Figure 8, for $W_2 = 0.42$ to $W_2 = 0.80$, but not the phase inversion.*

Equilibrium swelling of the unsubstituted IPNs and a theoretical analysis using eqs. (1) and (2) addressed the questions of network I domination and the addition of new physical crosslinks during IPN formation. Although the analysis could not conclusively support the concept of network I domination in the equilibrium swollen state, the electron micrographs indicated that polymer I formed the more continuous phase through most of the composition range in the dry state. In the swollen state, it was further demonstrated that no added physical or chemical crosslinks substantially exist.

The bulk properties of the IPNs can be analyzed with a crossplot of modulus versus composition of the DMS data at 120°C (see Fig. 7). The result is shown in Figure 10. The data were analyzed in terms of the Takayanagi models.[44] The solid line, indicating equal cocontinuity of polymers I and II, results from the equation

$$E = (1 - \lambda)E_{\mathrm{I}} + \lambda E_{\mathrm{II}} \tag{10}$$

The dashed line follows the equation

* Equation (6) gave domain sizes on the order of 15 nm (150 Å), depending on the exact composition. However, values of K for the ionomeric system seemed very uncertain,[47] and hence the simplified form, eq. (7), in which K is eliminated algebraically, was employed.

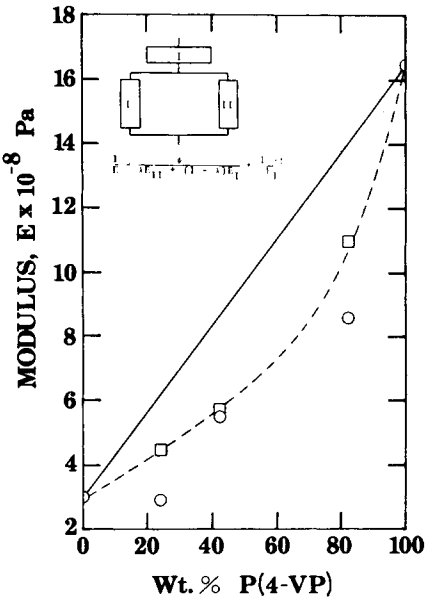

Fig. 10. Theoretical predictions using the Takayanagi model, eq. (11), shown and the E' data from Fig. 7 at 120°C. Circles represent experimental data at 120°C, and squares represent theoretical predictions.

$$\frac{1}{E} = \frac{\phi}{\lambda E_{II} + (1 - \lambda)E_I} + \frac{1 - \phi}{E_I} \tag{11}$$

which assumes polymer II is discontinuous (see inset, Fig. 10).[44] Since the data lie even below the dashed line, this analysis indicates the greater continuity of polymer I in space, in conformity with the electron micrographs, and the "dominance" of polymer I in such properties as modulus in the bulk state. An alternate Takayanagi model,[44] following the equation

$$E = \lambda\left[\frac{\phi}{E_{II}} + \frac{(1 - \phi)}{E_I}\right]^{-1} + (1 - \lambda)E_I \tag{12}$$

produced results nearly identical to those shown in Figure 10. In addition, analysis of the DMS data at 110 and 130°C yielded similar results, using both models.

Swelling of the ionomeric IPNs as a function of pH showed that sulfonated PS swelled to a greater extent than quaternized P(4-VP) at all pH values but exhibited a maximum in swelling at an approximately neutral pH. The presence of NaCl in the solvent significantly altered the swelling behavior but still showed the PS to swell preferentially. However, this area requires further investigation to determine the exact nature of the polymer–solvent and acid–base interactions due to the presence of the ionic groups.

Finally, these results may be considered in the light of the ultimate goal of the program, which is to develop a membrane suitable for piezodialysis. Piezodialysis is a novel desalination technique, in which salt is transported preferentially across the membrane and removed from a feed using pressure as the driving force.[27,43,45] The theory requires the membrane to consist of two continuous

phases, one anionic and one cationic.[46] A suitable material should have dual-phase continuity, but with a minimum of molecular mixing between the phases. Morphological features typical of IPNs seemed to fit the theoretical requirements. As shown by the electron micrographs, particularly Figures 8(b), 8(c), 8(f), and 8(g), the PS/P(4-VP) IPNs with midrange compositions appeared to possess a significant degree of the required dual-phase continuity. However, the DMS studies show that the present PS/P(4-VP) IPNs have probably more molecular mixing than desired.

It must be emphasized that the sequential IPN synthesis described herein makes a deliberate effort to avoid polyelectrolyte complex formation.[47] The coacervation that accompanies polyelectrolyte complex formation causes a single-phase product to be formed. By making the incompatible sequential IPN first, two separate phases are formed which are locked into separate regions of space via the crosslinks. Introduction of the ionic groups later in time minimizes polyelectrolyte complex formation.

The authors wish to thank the National Science Foundation for support through Grant No. ENG77-09097 A01.

References

1. H. L. Frisch, K. C. Frisch, and D. Klempner, *Mod. Plast.*, **54,** 76, 84 (1977).
2. J. A. Manson and L. H. Sperling, *Polymer Blends and Composites*, Plenum, New York, 1976, Chap. 8.
3. Y. S. Lipatov and L. M. Sergeeva, *Russ. Chem. Rev.*, **45**(1), 63 (1976).
4. D. A. Thomas and L. H. Sperling, in *Polymer Blends*, D. R. Paul and S. Newman, Eds., Academic, New York, 1978.
5. V. Huelck, D. A. Thomas, and L. H. Sperling, *Macromolecules*, **5**, 340, 348 (1972).
6. B. N. Kolarz, *J. Polym. Sci., Polym. Symp.* **47,** 197 (1974).
7. R. E. Touhsaent, D. A. Thomas, and L. H. Sperling, *J. Polym. Sci. Part C*, **46,** 175 (1974).
8. N. Devia, J. A. Manson, L. H. Sperling, and A. Conde, *Macromolecules*, **12,** 360 (1979).
9. G. C. Meyer and P. Y. Mehrenberger, *Eur. Polym. J.*, **13,** 383 (1977).
10. S. C. Kim, D. Klempner, K. C. Frisch, H. L. Frisch, and H. Ghiradella, *Polym. Eng. Sci.*, **15,** 339 (1975).
11. L. H. Sperling, *J. Polym. Sci., Polym. Symp.*, **60,** 175 (1977).
12. C. B. Bucknall and T. Yoshi, *Br. Polym. J.*, **10,** 53 (1978).
13. P. J. Flory and J. Rehner, *J. Chem. Phys.*, **11,** 512 (1943).
14. (a) J. L. Thiele and R. E. Cohen, *Polym. Prepr., Am. Chem. Soc., Div. Polym. Chem.*, **19**(1), 137 (1978); (b) *Polym. Eng. Sci.*, **19,** 284 (1979).
15. D. L. Siegfried, D. A. Thomas, and L. H. Sperling, *Macromolecules*, **12,** 586 (1979).
16. A. V. Galanti and L. H. Sperling, *Polym. Eng. Sci.*, **10,** 177 (1970).
17. A. V. Tobolsky and M. C. Shen, *J. Appl. Phys.*, **37,** 1952 (1966).
18. M. C. Shen, T. Y. Chen, E. H. Cirlin, and H. M. Gebhard, in *Polymer Networks: Structure and Mechanical Properties*, A. J. Chompff and S. Newmann, Eds., Plenum, New York, 1971.
19. Y. S. Lipatov, L. M. Sergeeva, L. V. Mozzhukhina, and N. P. Apukhtina, *Vysokomol. Soedin., Ser. A*, **16,** 2290 (1974).
20. L. H. Sperling and E. N. Mihalakis, *J. Appl. Polym. Sci.*, **17,** 3811 (1973).
21. A. Eisenberg and M. King, *Macromolecules*, **4,** 204 (1971); *Rubber Chem. Technol.*, **45,** 9081 (1972).
22. R. H. Kinney, *Appl. Polym. Symp.*, **11,** 77 (1969).
23. E. P. Otocka and T. K. Kwei, *Macromolecules*, **1,** 401 (1968).
24. W. J. MacKnight, *Polym. Prepr., Am. Chem. Soc., Div. Polym. Chem.*, **14**(2), 813 (1973).
25. G. S. Solt, Br. Pat. 728,508 (1955).
26. R. Longworth, in *Ionic Polymers*, L. Holliday, Ed., Wiley, New York, 1975.
27. L. H. Sperling, V. A. Forlenza, and J. A. Manson, *J. Polym. Sci., Polym. Lett. Ed.*, **13,** 713 (1975).
28. R. S. Drago, G. C. Vogel, and T. E. Needham, *J. Am. Chem. Soc.*, **93,** 6014 (1971).

29. D. A. Thomas, *J. Polym. Sci., Polym. Symp.*, **60,** 189 (1977).
30. C. L. Marx, J. A. Koutsky, and S. L. Cooper, *J. Polym. Sci., Polym. Lett. Ed.*, **9**, 167 (1971).
31. K. Kato, *J. Polym. Sci., Part B* **4**, 35 (1966).
32. K. Kato, *Polym. Eng. Sci.*, **7,** 38 (1967).
33. M. Pineri, C. Meyer, and A. Bourret, *J. Polym. Sci., Polym. Phys. Ed.*, **13,** 1881 (1975).
34. C. T. Meyer and M. Pineri, *Polymer,* **17,** 382 (1976).
35. P. J. Phillips, *J. Polym. Sci., Polym. Lett. Ed.*, **10,** 443 (1972).
36. A. A. Donatelli, L. H. Sperling, and D. A. Thomas, *Macromolecules,* **9,** 671 (1976).
37. A. A. Donatelli, L. H. Sperling, and D. A. Thomas, *J. Appl. Polym. Sci.*, **21,** 1189 (1977).
38. M. Matsuo, C. Nozaki, and Y. Jyo, *Polym. Eng. Sci.*, **9,** 197 (1969).
39. M. Matsuo, *Jn. Plast.*, **2,** 6 (1969).
40. G. Kraus and K. W. Rollman, in *Multicomponent Polymer Systems,* N. A. J. Platzer, Ed., *Adv. Chem. Ser. 99,* ACS, Washington, D.C., 1971.
41. P. R. Scarito and L. H. Sperling, *Polym. Eng. Sci.*, **19,** 297 (1979).
42. ASTM D1043-72, in Part 27, *Annual Book of ASTM Standards,* ASTM, Philadelphia, 1974.
43. G. Lopatin and H. A. Newey, in *Reverse Osmosis Membrane Research,* H. K. Lonsdale and H. E. Podall, Eds., Plenum, New York 1972.
44. M. Takayanagi, H. Harima, and Y. Iwata, *Mem. Fac. Eng., Kyusha Univ.*, **23,** 1 (1963).
45. U. Merten, *Desalination,* **1,** 297 (1966).
46. O. Kedem and A. Katchalsky, *Trans. Faraday Soc.*, **59,** 1918, 1931, 1941 (1963).
47. M. J. Lysaght, in *Polyelectrolytes,* K. C. Frisch, D. Klempner, and A. V. Patsis, Eds., Technomic, Westport, CT, 1976.

Received June 12, 1979
Revised September 13, 1979